Automated Classification of Operational SAR Sea Ice Images

Shuhrat Ochilov and David A. Clausi
Vision and Image Processing (VIP) Research Group
Systems Design Engineering, University of Waterloo
Waterloo, ON, Canada
{*sochilov, dclausi*}@*engmail.uwaterloo.ca*

Abstract

The automated classification of operational sea ice satellite imagery is important for ship navigation and environmental monitoring. Annually, thousands of large synthetic aperture radar (SAR) scenes are manually processed by the Canadian Ice Service (CIS) and pixel-level interpretation is not feasible. Trained ice analysts divide SAR images into "polygon" areas and then identify the number and type of ice classes per polygon. Full scene unsupervised classification can be performed by first segmenting each polygon into distinct regions algorithmically. Since there is insufficient information to assign a sea ice label for each region within an individual polygon, a Markov random field formulation using joint information to label each region in a full SAR scene has been developed. This approach has been successfully applied to operational CIS data to produce pixel-level classified images and is the first known successful end-to-end process for automatically classifying operational SAR sea ice images.

1. Introduction

Spaceborne synthetic aperture radar (SAR) has been used operationally for sea ice monitoring applications such as climate research and ship navigation. Currently, SAR sea ice images are manually analyzed by sea ice experts to provide clients with a coarse ice map. According to the Canadian Ice Service (CIS), approximately four thousand 10Kx10K RADARSAT-1 (a Canadian SAR satellite) images are processed every year [6]. Manual pixel-level interpretation of SAR sea ice images is not feasible and an automated approach is desired.

Methods have been proposed which try to classify SAR sea ice imagery by mapping every pixel directly to sea ice types using the statistics from training samples [1, 3, 4, 10, 18]. The features corresponding to same ice type vary according to various environmental and sensor conditions making training samples unreliable even within scene. Hence, the classification techniques relying on the thresholds and statistics derived from training samples [19, 22] might not perform well for operational use. The solution might be the investigation of features and statistics that have common characteristics over all sea ice scenes or extracting features from samples obtained from the images themselves by initial unsupervised segmentation. The last option has been adapted in this research and the sea ice classification is performed in two stages: unsupervised segmentation followed by sea ice labeling.

Several techniques have been proposed to automatically segment SAR sea ice scenes into disjoint regions [5, 9, 17, 20, 23]. Among these, IRGS [23] has shown outstanding performance segmenting both operational SAR sea ice and general purpose imagery. The segmentation technique has been successfully tested and CIS validated using a variety of SAR sea ice images. IRGS has also evolved into a software system called MAGIC [5] to use CIS source data and enable consistent testing in an easy-to-use GUI framework. For these reasons IRGS has been used as the segmentation algorithm in our research.

Although tremendous progress has been made on SAR sea ice segmentation, limited research has been performed on ice type labeling and the initial attempts [13] provide classification results which are locally optimal in nature. To obtain the classification result which is optimal over the whole scene, labeling can be performed automatically using information from all polygons simultaneously.

Operational processing of SAR sea ice imagery is summarized in Fig. 1. The first step as shown in Fig. 1(a) is image acquisition by RADARSAT- 1,2 satellites. A CIS sea ice analyst manually divides the image into polygon regions, referred to as polygons, as shown in Fig. 1(b) and just reports the sea ice types that exist in each polygon. To automatically classify images based on metadata provided by sea ice analyst, unsupervised segmentation using IRGS can be performed on every polygon independently to produce Fig. 1(c). The challenge is to assign a sea ice label

978-0-7695-4040-5/10 $26.00 © 2010 IEEE
DOI 10.1109/CRV.2010.59

to each segmented region in each polygon across the entire SAR scene as per Fig. 1(d). Subsequently, this research focuses on solving this labeling problem utilizing information from the full scene.

The novel sea ice labeling technique is proposed which seeks a global solution over the full SAR scene. The proposed approach uniquely models the spatial relationship of regions between the polygons in the form of new polygonal neighborhood system embedded in a Markov random field (MRF) framework [2]. As such, region labeling is formulated as an energy minimization problem. Energy is a global metric over the full SAR sea ice scene utilizing information from all polygons. Energy minimization is achieved using the optimization with Metropolis sampling [15] to accommodate the idea that the labeling state of the regions of the polygon is one of the permutations of assigned labels to that polygon. This definition is derived from the fact that the ice types in each polygon are provided by the analyst. The operational side of the proposed framework is that no training samples are required and that the domain knowledge is solely based on the metadata provided by the analyst in step Fig. 1(b).

The rest of the paper is organized as follows. Section 2 describes sea ice labeling model. Section 3 includes the methodology for solving the objective function and selecting parameters. The performance of the proposed algorithm using operational SAR sea ice imagery of Arctic region is investigated in Section 4. Final remarks are included in Section 5.

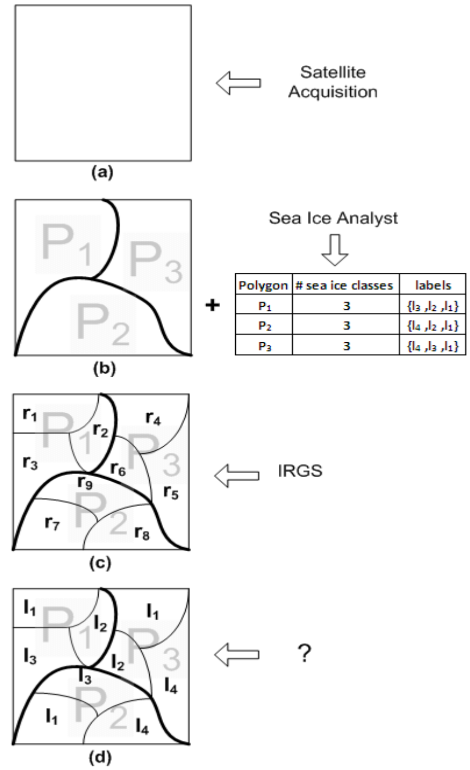

Figure 1. Classification of full scene operational SAR sea ice images. r, P ,l refer to region, polygon and sea ice label, respectively. (a) Original SAR image. (b) Image manually divided into polygons with appropriate ice type metadata. (c) Image with every polygon automatically segmented into regions using IRGS [23]. (d) Image with every region automatically labeled with sea ice type. This paper focuses on (d), the labeling problem.

2. Sea Ice Labeling Model

2.1 Definitions

Let S denote a discrete 2D rectangular image space of size $M \times N$. $X = \{X_s | s \in S\}$ represents the random field defined on S, where X_s is the random variable representing the grey tone or the multivariate feature. The segmented image $Y = \{Y_s | s \in S\}$ is another univariate 2D image space defined on S where each discrete valued random variable Y_s, having a value in $\{1, \dots n_r\}$, represents the region to which the site s belongs. Suppose there are n_l different sea ice classes in Y. Let $Z = \{Z_s | s \in S\}$ be another 2D random field defined on S where each discrete valued random variable Z_s, having a value in $\{1, \dots n_l\}$, represents the sea ice classes to which site s belongs. Suppose the realization of Z is $z = \{z_s | s \in S\}$, then the sea ice labeling problem can be formulated as an estimation of z from y and x:

$$L : \left\{ \begin{array}{l} \{x_s | s \in S\} \\ \{y_s | s \in S\} \end{array} \right. \longrightarrow \{z_s | s \in S\} \qquad (1)$$

Definitions essential to the proposed classification model are given next.

Definition 1: *A graph G* $:= (r, \partial)$ consists of *regions* $r = \{r_1, r_2, \dots, r_{n_r}\}$ having boundaries $\partial r_{ij} = \{s, t | s \in r_i, t \in r_j, t \in N_s\}$ where N_s is defined as first-order neighborhood of site s.

Definition 2: Two regions r_i, r_j are *neighbors* if and only if $\partial r_{i,j} \neq \emptyset$. N_{r_i} is the *neighborhood* of a region r_i comprising all regions r_j for which r_i, r_j are neighbors and has a symmetrical relationship $r_j \in N_{r_i} \Leftrightarrow r_i \in N_{r_j}$. *Neighborhood system* N_r is set of all neighborhoods.

Definition 3: Two regions r_i, r_j are *polygonal neighbors* if and only if $\partial r_{i,j} \neq \emptyset$ and $r_i, r_j \not\subseteq P_q$ for some polygon P_q.

N_{p_i} is the *polygonal neighborhood* of a region r_i comprising all regions r_j for which r_i, r_j are polygonal neighbors and has symmetrical relationship $r_j \in N_{p_i} \Leftrightarrow r_i \in N_{p_j}$. *Polygonal neighborhood system* N_p is a set of all polygonal neighborhoods.

Constraint 1: The labeling realization $\{z_s | s \in P_q\}$ of some polygon P_q is constrained to one of the permutations of sea ice classes given for that polygon.

2.2 Feature energy model

The statistical nature of SAR images indicates that the amplitude of the scattered signal is gamma distributed, however, in-house testing and published research [21] indicate that modeling features as a Gamma mixture produces segmentation results comparable to Gaussian mixtures. Thus, for simplicity, features are assumed to be Gaussian mixture modeled and the region energy of K dimensional features is defined as:

$$\begin{aligned} E(r_i) &= \sum_{s \in r_i} \frac{1}{2} \ln(2\pi)^K |\Sigma_{l_{r_i}}| \\ &+ \frac{1}{2}(x_s - u_{l_{r_i}})^T {\Sigma_{l_{r_i}}}^{-1} (x_s - u_{l_{r_i}}) \end{aligned} \quad (2)$$

here $u_{l_{r_i}}$,$\Sigma_{l_{r_i}}$ are the mean and covariance of the class having same label as region r_i. $|\Sigma_{l_{r_i}}|$ is the determinant of the covariance matrix and T is the transpose operation. The energy of a region in Eq. 2 is the sum of the energies of all sites s belonging to that region. The total energy E_f over all regions is:

$$E_f = \sum_{i=1}^{n_r} E(r_i) \quad (3)$$

2.3 Pairwise node clique energy

The pairwise clique potential which is used to model the spatial context is expressed as:

$$V_2(r_i, r_j)_{(r_i, r_j) \in N_P} = \begin{cases} \beta g(\nabla_{r_i, r_j}) & l_{r_i} \neq l_{r_i} \\ 0 & l_{r_i} = l_{r_j} \end{cases} \quad (4)$$

where β is the weight for spatial model and l_{r_i} and l_{r_j} are the labels assigned to r_i, r_j respectively.

$$g(\nabla_{r_i, r_j}) = 1 - \nabla_{r_i, r_j} \quad (5)$$

is the edge penalty term with the edge strength

$$\nabla_{r_i, r_j} = \sum_{s,t \in \partial r_{i,j}} |x_s - x_t| \quad (6)$$

normalized to the range $[0 \ldots 1]$. Using the Eq. 4 and the total energy for the regional interactions can be derived as:

$$E_r = \sum_{r_i, r_j \in N_r} V_2(r_i, r_j) \quad (7)$$

The regions in the same polygon are never assigned the same label and based on the fact that β is constant inter polygon pairwise clique energies $\beta g(\nabla_{r_i, r_j}) r_i, r_j \nsubseteq P_q$ have no effect in energy minimization process. Thus, the total energy for the regional interactions is:

$$E_r = \sum_{r_i, r_j \in N_P} V_2(r_i, r_j) \quad (8)$$

2.4 Energy Minimization

Subsequently, the MAP estimation derived from Bayesian theory is the estimator which tries to maximize the *a posteriori* probability. The labeling is achieved in the following section by first estimating the parameters and then by minimizing the total energy:

$$\arg \min_{\{z_s | s \in S\}} (\alpha E_f + \beta E_r) \quad (9)$$

3. Optimization and Parameter Estimation

To optimize Eq. 9 the combination of simulated annealing (SA) and Metropolis sampling has been applied which uses a commonly used temperature schedule [16].

There are four parameters to be estimated: $u_{l_{r_i}}$, $\Sigma_{l_{r_i}}$, α and β. Since no training data is provided and the segmentation is unsupervised, the EM [24, 7] algorithm can be used for estimating $u_{l_{r_i}}$,$\Sigma_{l_{r_i}}$, mean and covariance, parameters for every class to which regions r_i belong. EM is suitable for maximum likelihood estimation of feature parameters of incomplete data [24] and the convergence of the EM algorithm is known [14].

Here, β is set to one and the parameter α needs to be estimated accordingly. In conventional multi-level logistic (MLL) models [12], α is selected to be constant leading to solution divergence in early stages due to too much weighting of the spatial context model. To deal with this problem, the feature and spatial model relative weights can vary with each iteration [8]. In this research, the same approach is followed to determine α. As such, the parameter α can vary according to:

$$\alpha(\theta) = c_1\, 0.9^{\theta} + c_2 \quad (10)$$

where c_1, c_2 are constants equal to 0.1. Eq. 10 monotonically decreases α with each iteration θ.

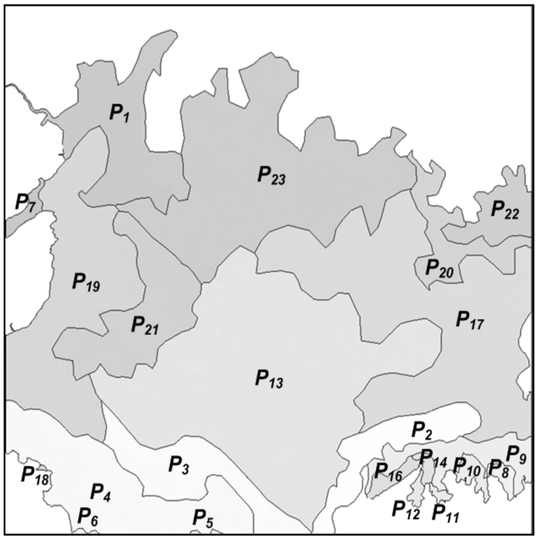

(a)

Figure 2. Polygons of full SAR sea ice scene in Fig. 3(a)

Table 1. Metadata for Fig. 2. Using the World Meteorological Organization (WMO) standard [11], labels refer to new ice (1), grey ice (4), grey white ice (5), multiyear ice (9), and fast ice (L)

Polygon	$\#iceclasses$	labels
P_1	3	$\{5,4,1\}$
P_2	2	$\{4,1\}$
P_3	3	$\{5,4,1\}$
P_4	3	$\{9,5,4\}$
P_5	2	$\{4,1\}$
P_6	3	$\{9,5,4\}$
P_7	2	$\{4,1\}$
P_8	2	$\{L,5\}$
P_9	3	$\{L,4,1\}$
P_{10}	2	$\{L,5\}$
P_{11}	2	$\{L,5\}$
P_{12}	2	$\{L,5\}$
P_{13}	3	$\{5,4,1\}$
P_{14}	3	$\{L,5,4\}$
P_{15}	3	$\{L,5,4\}$
P_{16}	3	$\{5,4,1\}$
P_{17}	2	$\{4,1\}$
P_{18}	3	$\{9,5,4\}$
P_{19}	2	$\{4,1\}$
P_{20}	3	$\{5,4,1\}$
P_{21}	2	$\{4,1\}$
P_{22}	2	$\{4,1\}$

4. Experimental Results

4.1. SAR Sea Ice Image

Using the technique described in Section 3, sea ice labeling was performed on an operational SAR sea ice scene. The image in Fig 3(a) is the SAR sea ice scene of Arctic region with latitude/longtitude ranges of $\{69.7270°, 76.9649°\}/\{-80.5216°, -66.0010°\}$ and has been acquired by the RADARSAT-1 satellite in ScanSAR mode on October 30, 2005. For image archival and for testing purposes, CIS applies 2x2 block averaging which corresponds to a pixel resolution of 100m and to an image size of 5008x5387 pixels in our case. The SAR scene with overlaid operator drawn polygons is depicted in Fig. 2 and the corresponding polygon metadata as generated by an operator is listed in Table 3. The unsupervised segmentation with IRGS shown in Fig 3(b) is arbitrarily colored, since displaying in grey-scale does unavoidably reduce segmentation details.

4.2. Testing

Fully validated field ground truth for the operational SAR sea ice image is not available. For unequivocal validation, one would have to perform judicious field sampling of the sea ice on site across a 500km by 500km region during the SAR satellite overpass. Due to the logistical impossibility of such a validation exercise, we instead rely on the decades of CIS experience and know-how for interpreting SAR imagery for validation purposes. As such, the segmentation and labeling results presented here have been validated by a trained SAR sea ice expert at CIS.

The proposed sea ice labeling algorithm has been applied to an IRGS segmented image Fig. 3(b) and the result displaying in Fig. 3(c) with more than 80% accuracy reported. The justification is the accurate localization and labeling of new ice, grey ice, grey white and multiyear ice types in the image. Misclassification might occur for any one of the following reasons.

1. The number of classes provided might be determined incorrectly by the ice analyst.

2. Ice analyst might be biased toward assigning thicker ice type in some polygons. This is due to erring on the side of caution with regards to providing products for ship routing.

3. Polygons are drawn manually so the boundaries are often imprecise and accidentally include ice types not recorded for a particular polygon.

4. The segmentation might fail over some complex scenarios resulting in incorrectly formed regions. For example, the ice type discrimination might depend on floe shape characteristics and not on the grey tone. The current segmentation algorithm relies on grey tone alone.

Note that most of the reasons for misclassification are based on operator error when generating the polygon regions. Generally, if the operator provided information is accurate (number of ice types, ice type labels, boundaries between polygons) then the segmentation has a stronger accuracy and the labeling process produces a more accurate pixel classified map.

To test the role of the spatial context model in the labeling process, we removed the E_r term from Eq. 9 to only consider the feature model term E_f. By removing the spatial context model, only the Gaussian mixture model (GMM) remains. The labeling result using GMM alone is illustrated in Fig. 3(d). In this case, half of the regions has been misclassified compared with the result in Fig. 3(c). This clearly indicates that the spatial interaction of polygons is essential in the overall model to generate accurate labeling.

To better evaluate and visualize classification results of proposed sea ice labeling technique the image in Fig. 3(c) has been transformed to a color image in Fig. 4 using World Meteorological Organization (WMO) standard codes [11].

5. Conclusions

An efficient method has been designed and implemented for full automatic classification of SAR sea ice images. In the classification process, the scene has been automatically segmented and operationally acceptable labeling result has been obtained. This is the only known end-to-end process for automatically segmenting and labeling operational SAR sea ice imagery. The algorithm uses the information from all polygonal regions and finds the optimal configuration of labels based on an objective function composed of both a feature model and spatial model. To demonstrate the functionality and the concept the results have been presented with an operational RADARSAT-1 image provided by CIS with corresponding operational metadata. The classification performance can be improved further by solving the existing limitations described in Section 4.2.

6. Acknowledgements

Acknowledgements are extended for support of this project by Geomatics for Informed Decisions (GEOIDE, an Network of Centres of Excellence under the Natural Sciences and Engineering Research Council) and CRYSYS (CRYospheric SYStem in Canada). CIS is thanked for their provision of operational SAR sea ice images. Sea ice analyst Thomas Zagon of CIS is thanked for validating the segmentation and labeling outcomes.

References

[1] D. G. Barber and E. F. LeDrew. SAR sea ice discrimination using texture statistics: A multivariate approach. *Photogrammetric Engineering and Remote Sensing*, 57(4):385–395, 1991.

[2] J. Besag. Spatial interaction and the statistical analysis of lattice systems. *Journal of the Royal Statistical Society*, 1974.

[3] A. V. Bogdanov, S. Sandven, O. M. Johannessen, V. Y. Alexandrov, and L. P. Bobylev. Multisensor approach to automated classification of sea ice image data. *IEEE Transactions on Geoscience and Remote Sensing*, 43(7):1648–1664, 2005.

[4] D. A. Clausi. Comparison and fusion of co-occurrence, Gabor and MRF texture features for classification of SAR sea-ice imagery. *Atmosphere and Oceans*, 39(3):183–194, 2001.

[5] D. A. Clausi, A. K. Qin, M. S. Chowdhury, P. Yu, and P. Maillard. MAGIC: Map-Guided Ice Classification System. In *Canadian Journal of Remote Sensing*, 2009.

[6] G. F. Dean, J. W. Katherine, W. V. Paris, and J. F. Hopper. Wind information for marine weather forecasting from RADARSAT-1 synthetic aperture radar data: Initial results from the Marine winds from SAR demonstration project. *Canadian Journal of Remote Sensing*, 28(3):490–497, 2002.

[7] A. P. Dempster, N. M. Laird, and D. B. Rubin. Maximum likelihood from incomplete data via the EM Algorithm. *Journal of the Royal Statistical Society*, pages 1–38, 1977.

[8] H. Deng and D. A. Clausi. Unsupervised image segmentation using a simple MRF model with a new implementation scheme. *Pattern Recognition*, 37(12):2323–2335, 2005.

[9] H. Deng and D. A. Clausi. Unsupervised segmentation of synthetic aperture Radar sea ice imagery using a novel Markov random field model. *IEEE Transactions on Geoscience and Remote Sensing*, 43(3):528–538, 2005.

[10] D. Haverkamp, L. K. Soh, and C. Tsatsoulis. A dynamic local thresholding technique for sea ice classification. In *IEEE International Geoscience and Remote Sensing Symposium (IGRRS'93)*, pages 638–640, 1993.

[11] http://www.wmo.int/. World meteorological organization website [online], March 2009.

[12] S. Z. Li. Markov random field modeling in computer vision. *Springer, New York*, 2001.

[13] P. Maillard, D. A. Clausi, and H. Deng. Map-guided sea ice segmentation and classification using SAR imagery and a MRF segmentation scheme. *IEEE Transactions on Geoscience and Remote Sensing*, 43(12):2940–2951, 2005.

[14] G. McLachlan and T. Krishnan. The EM algorithm and extensions. *Wiley and Sons, New York*, 1996.

[15] N. Metropolis, A. W. Rosenbluth, M. N. Rosenbluth, A. H. Teller, and E. Teller. Equations of state calculations by fast computing machines. *Journal of Chemical Physics*, 21(6):1087–1091, 1953.

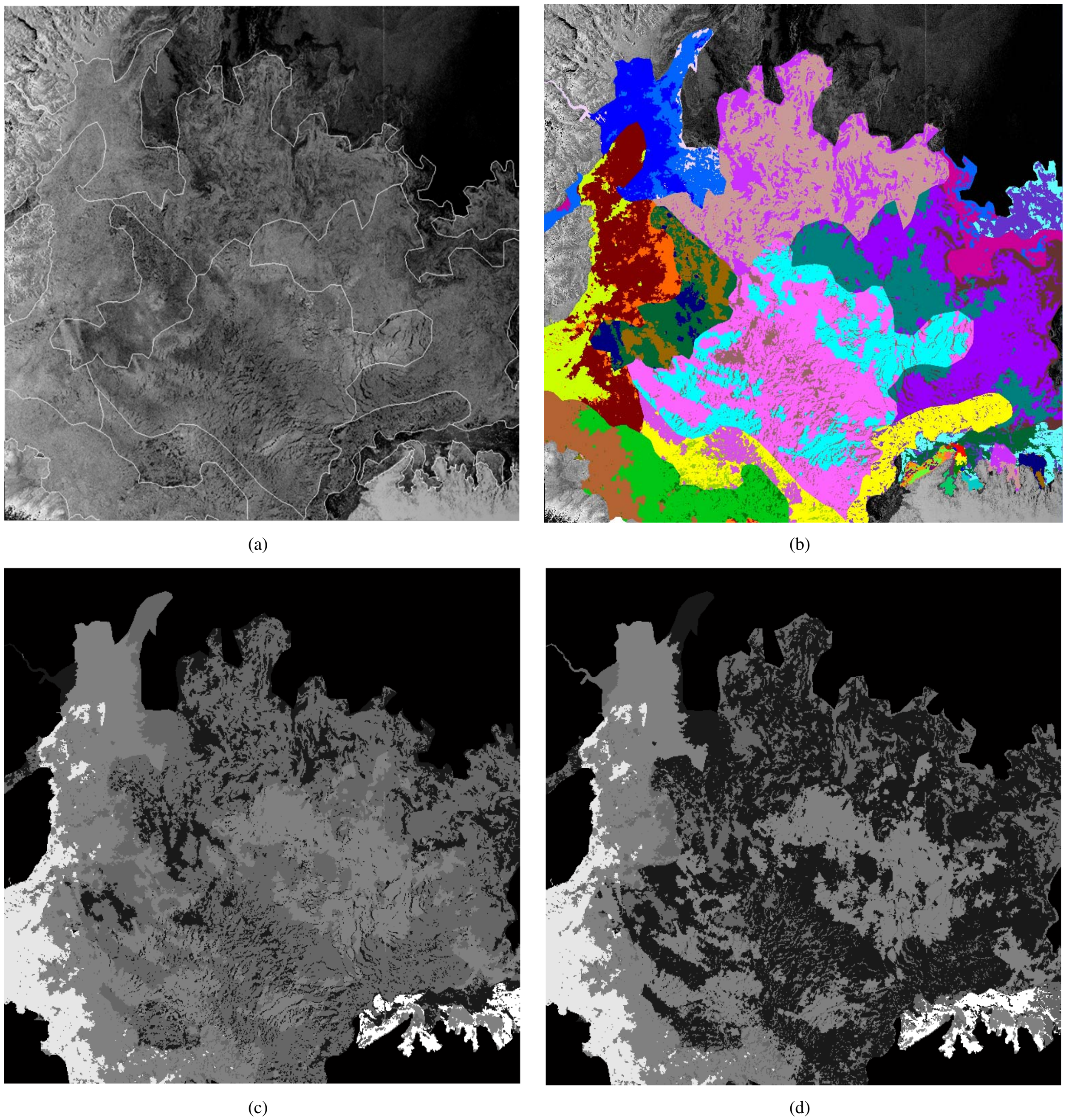

Figure 3. (a)Original full SAR sea ice scene of Arctic region (October 30, 2005). Polygon boundaries are overlaid on the image as white contours. (b) The unsupervised segmentation of image in (a) using IRGS. (c) The labeled output using the proposed algorithm with accuracy at least 80%. (d)The labeled output with using just the feature model represented by a Gaussian mixture model. Without the spatial context model, the labeling process produces poor results.

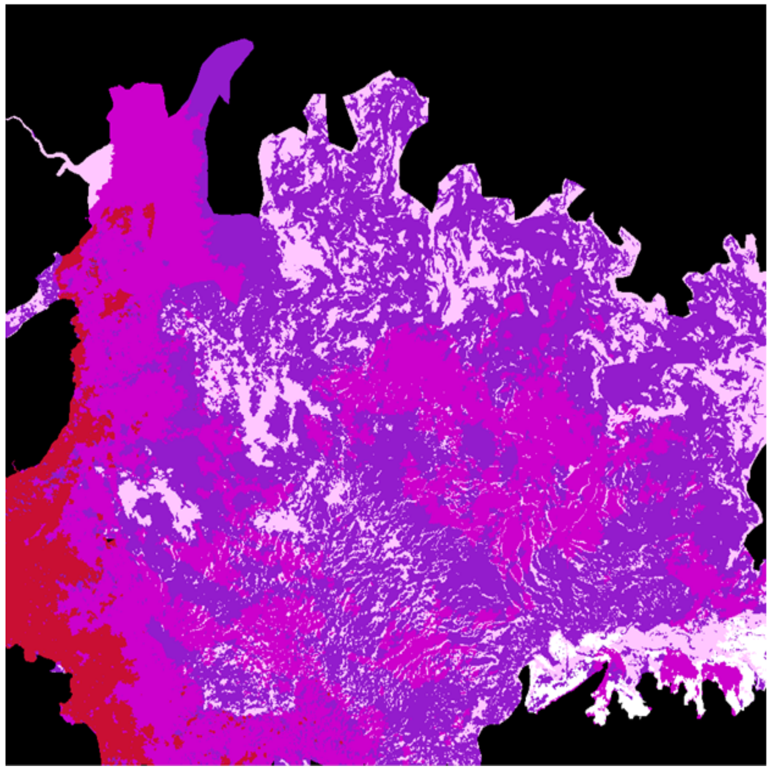

(a)

(b)

Figure 4. Classification result of Fig 3(c) using the WMO color code [11].

[16] D. G. S. Geman. Stochastic relaxation, Gibbs distributions, and the Bayesian restoration of images. *IEEE Transaction on Pattern Analysis and Machine Intelligence*, 6(6):721–741, 1984.

[17] R. Samadani. A finite mixtures algorithm for finding proportions in SAR Images. *IEEE Transaction on Image Processing*, 4(8):1182–1186, 1995.

[18] M. E. Shokr. Evaluation of second-order texture parameters for sea ice classification from radar images. *Journal of Geophysical Research*, 96:10625–10640, 1991.

[19] L. Soh, C. Tsatsoulis, D. Gineris, and C. Bertoia. ARKTOS: An intelligent system for SAR sea ice image classification. *IEEE Transactions on Geoscience and Remote Sensing*, 42(1):229–248, 2004.

[20] L. K. Soh and C. Tsatsoulis. Unsupervised segmentation of ERS and RADARSAT sea ice images using multiresolution peak detection and aggregated population equalization. 20(15):3087–3109, 1999.

[21] Q. Yu. *Automated SAR Sea Ice Interpretation.* PhD thesis, 2006.

[22] Q. Yu and D. A. Clausi. SAR sea-ice image analysis based on iterative region growing using semantics. *IEEE Transactions on Geoscience and Remote Sensing*, 45(12):3919–3931, 2007.

[23] Q. Yu and D. A. Clausi. IRGS: Image segmentation using edge penalties and region growing. *IEEE Transaction on Pattern Analysis and Machine Intelligence*, 30(12):2126–2139, 2008.

[24] J. Zhang. The mean field theory in EM procedures for Markov random fields. *IEEE Transactions on Signal Processing*, 40(10):2570–2583, 1992.